

A new method for quantitative analysis of mammographic density

Carri K. Glide-Hurst,^{a)} Neb Duric, and Peter Littrup

Karmanos Cancer Institute and Wayne State University, 110 East Warren, Hudson-Webber Cancer Research Center, Room 7040, Detroit, Michigan 48201

(Received 2 April 2007; revised 28 August 2007; accepted for publication 29 August 2007; published 29 October 2007)

Women with mammographic percent density $>50\%$ have a \sim three-fold increased risk of developing breast cancer, potentially making them screening candidates for breast MRI scanning. The purpose of this work is to introduce a new method to quantify mammographic percent density (MPD), and to compare the results with the current standard of care for breast density assessment. Craniocaudal (CC) and mediolateral oblique (MLO) mammograms for 104 patients were digitized and analyzed using an interactive computer-assisted segmentation routine implemented for two purposes: (1) to segment the breast area from background and radiographic markers, and (2) to segment dense from fatty portions of the breast. Our technique was evaluated by comparing the results to qualitative estimates determined by a certified breast radiologist using the BI-RADS Categorical Assessment (1 (fatty) to 4 (dense) scale). Statistically significant correlations (two-tailed, $p < 0.01$) were observed between calculated MPD and BI-RADS for both CC (Spearman $\rho = 0.67$) and MLO views (Spearman $\rho = 0.71$). For the CC view, statistically significant differences were revealed between the mean MPD for each BI-RADS category except between fatty (BI-RADS 1) and scattered (BI-RADS 2). Finally, for the MLO views, statistically significant differences in the mean MPD between all BI-RADS categories were observed. Comparing the CC and MLO views revealed a strong positive correlation (Pearson $r = 0.8$) in calculated MPD. In addition, an evaluation of the reproducibility of our segmentation demonstrated the average standard deviation of MPD for a subsample of eight patients, measured five times, was 1.9% (range: 0.03%–9.9%). Eliminating one misassignment reduced the average standard deviation to 0.75% (range: 0.03%–3.16%). Further analysis of $\sim 10\%$ of the patient sample revealed strong agreement (ICC = 0.80–0.85) in the reliability of MPD estimates for both mammographic views. Overall, these results demonstrate the feasibility of utilizing our approach for quantitative breast density segmentation, which may be useful for detecting small changes in MPD introduced through chemoprevention, diet, or other interventions. © 2007 American Association of Physicists in Medicine. [DOI: [10.1118/1.2789407](https://doi.org/10.1118/1.2789407)]

Key words: mammographic breast density, segmentation, BI-RADS

I. INTRODUCTION

Mammographically dense breast tissue is strongly associated with an increase in breast cancer risk, with a relative risk of up to four to five times more for women with dense breasts.^{1–4} Furthermore, increased breast density has been shown to be more prognostic of overall breast cancer risk than nearly all other risk factors.^{5–7} The American Cancer Society therefore recommends that women with a calculated lifetime risk of breast cancer $>20\%$ receive screening MRI.⁸ A recent detailed analysis of breast density levels not only confirmed previous breast cancer risk estimates, but also clearly placed a \sim three-fold increased risk of breast cancer for patients with overall density $>50\%$.⁴ Should breast density become an important component of risk assessment models as recent studies have suggested,^{9–11} an objective breast density estimation may be used to identify women who are more likely to be eligible for MRI screening. However, current breast density estimation is not readily quantified in such a manner for broad community application or acceptance.

Breasts are comprised of both fat—a radiolucent material—and fibroglandular tissue, and as a result of this

distribution, the mammographic percent density (MPD) can be calculated to represent the ratio of fibroglandular to total breast areas. Typically, MPD is assessed by radiologists who score the breast composition into one of four different BI-RADS categories: (1) almost entirely fat ($<25\%$ glandular), (2) scattered fibroglandular (25%–50% glandular), (3) heterogeneously dense (51%–75% glandular), and (4) extremely dense ($>75\%$ glandular). The American College of Radiology has established these BI-RADS categories as the current standard of care in breast density reporting.¹² While this approach is quick and cost-effective to implement, the use of BI-RADS categories is not ideal because of considerable intra- and inter-reader variability.^{13,14}

To address these limitations, several investigators have developed computer-aided segmentation algorithms to calculate mammographic density from digitized mammograms.^{15–17} However, these techniques require the user to interactively select global threshold values for the background and/or dense tissue area, which introduces the potential for additional user variability. In addition, previous research has tended to evaluate craniocaudal (CC) mammograms despite the fact that mediolateral (MLO) views evalu-

TABLE I. The BI-RADS compositional category distribution for our patient population.

BI-RADS compositional category	Patient sample (% of population)
(1) Fatty (<25%)	11 (11%)
(2) Scattered (26%–50%)	66 (63%)
(3) Heterogeneous (51%–75%)	19 (18%)
(4) Dense (>75%)	8 (8%)

ate a greater extent of breast tissue. This may be because CC views do not typically require pectoral muscle segmentation. The method we are presenting, however, automates the segmentation of the breast from background, and semiautomates the segmentation of pectoral muscle and fibroglandular tissue from the rest of the breast. As an independent evaluation of our technique, we segmented both CC and MLO digitized mammograms for each patient, and compared them to BI-RADS categorical assessments. Finally, we compared the segmentation results between MLO and CC views and evaluated the reproducibility of our technique. The results of this study introduce a novel means of breast density evaluation, which may be used to identify women who are at high risk for breast cancer and as a result are eligible for future screening MRI.

II. METHODS AND MATERIALS

II.A. Patient sample and BI-RADS classification

Patients in this study were recruited from the Walt Comprehensive Breast Center located at Karmanos Cancer Institute at Wayne State University. All imaging procedures were performed under an institutional review board approved protocol and in compliance with the Health Insurance Portability and Accountability Act. The patient population included 104 case sets and provided a variety of breast sizes and densities, with a median patient age of 48.5 years (range, 21–85).

As an independent evaluation of our methodology, we compared our results with BI-RADS categories defined by a radiologist (P.L.) board-certified in mammographic interpretation with over 10 years of breast imaging experience. The radiologist also used the descriptive pictorials displayed in the BI-RADS Breast Imaging Atlas for consistent evaluation standards.¹² The resulting sample distribution is shown in Table I. The majority of the sample was distributed in the two intermediate categories, which is consistent with the findings from previous studies.^{18,19}

II.B. Image digitization and processing

Mammograms in the CC and MLO projections were digitized using a Vidar VXR-16 Dosimetry Pro digitizer with a TWAIN interface (version 5.2.1). The digitization parameters utilized were as follows: 71 dpi resolution, 8 bit depth, and the application of a logarithmic translation table. High resolution images are not required for MPD calculation because this ratio is known to be a coarse measure.²⁰

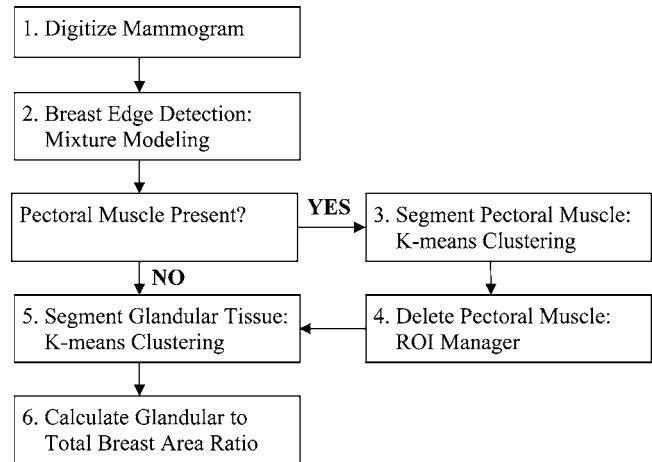


FIG. 1. Flowchart that demonstrates the algorithm used in segmentation of mammograms. For the majority of the craniocaudal mammograms, the chest wall did not need to be removed and steps 3 and 4 were omitted for these cases.

An interactive, computer-assisted segmentation routine was implemented for mammogram segmentation. Figure 1 demonstrates the algorithm followed for MPD calculation for the MLO view. All image analysis procedures were performed using IMAGEJ (available at: <http://rsb.info.nih.gov/ij/download.html>).²¹ First, to segment the breast area from background and radiographic markers, a mixture-modeling algorithm was employed (available at: <http://rsb.info.nih.gov/ij/plugins/mixture-modeling.html>).²² This algorithm separated the gray-level histogram of an image into two different classes (i.e., breast and nonbreast features) using Gaussian modeling. The first Gaussian curve modeled the prominent background peak, while the second peak was fit to the other features. The threshold intersection is automatically calculated based on a multistep process. First, the gray-level histogram is scanned, two mean gray-level values are calculated, and the error between the two mean values is minimized. The threshold intersection is then further optimized by iteratively fitting two weighted Gaussians to the data. The minimized error between these two fits provides the intersection threshold for the mammogram, which is then used to create the binary mixture-modeled image (shown in Fig. 2(B)).

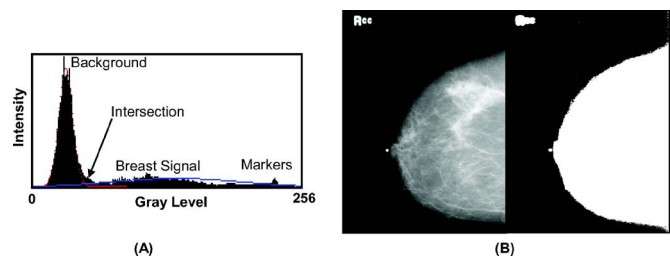


FIG. 2. (A) The mixture modeling algorithm fits two Gaussians to the gray-level histogram of the mammogram. The intersection of the Gaussians distinguishes the breast signal from the background. (B) Craniocaudal mammogram (BI-RADS Category 1, Fatty) with the breast edge defined by the mixture modeling technique.

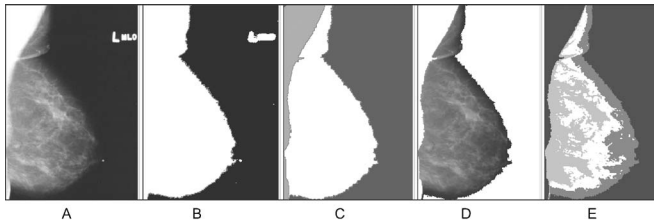


FIG. 3. (A) Left medio-lateral mammogram. (B) The breast edge defined by the mixture modeling technique. (C) k -means clustering of the chest wall from the breast. (D) Total breast area with chest wall segmented. (E) Dense area (light gray) segmented from the remaining breast area using k -means clustering. The mammographic percent density was calculated by dividing the dense area (light gray in (E)) by the entire breast area shown in (D).

The breast outline is automatically selected using the tracing tool which traces the breast edge on the binary image. This region of interest was saved to IMAGEJ's ROI Manager, which records the current ROI selection, image number, and x and y coordinates of the selection. This ROI was then restored onto the original mammogram using the ROI Manager and the exact recorded coordinates. The areas outside of the breast outline (i.e., background, radiographic markers, and labels) were deleted using the "Clear Outside" function, which erases the area outside of the selection and sets the erased area to the background gray-level value. The tracing tool, ROI Manager, and Clear Outside function are all built-in components of IMAGEJ and do not need to be downloaded.

Once the background and radiographic markers were eliminated, the third step was to segment the chest wall from the breast by employing a k -means clustering routine (Fig. 3(C)). The k -means clustering routine is an IMAGEJ plug-in (available at: http://sourceforge.net/project/showfiles.php?group_id=44711&package_id=37246). k -means clustering employs pixel-based segmentation where each cluster (n) is defined by its centroid in n -dimensional space. Cluster centroids are established using heuristics, and pixels are then segregated according to their proximity to the cluster's centroid values.²³ Further information on data clustering can be found in Ref. 24.

Next, the user was required to define the number of clusters used in the k -means clustering segmentation of the chest wall. As Fig. 3(A) shows, the highly attenuating regions associated with the chest wall and pectoral muscle are clearly visible at the edge of the mammogram. Upon quick visual inspection, the operator should be able to easily decipher if the high intensity regions near the chest wall region are a natural part of the breast area, or if they should be segmented out to avoid being included in the calculation of breast density. The high intensity chest wall regions on a mammogram are clearly demarcated from the rest of the breast using the k -means clustering technique, as demonstrated by Fig. 3(C). Once the background has been deleted with the mixture-modeling method, two or three clusters are typically used to segment the pectoral muscle from the rest of the breast. Once the chest wall was segmented, the region of interest was superimposed on the breast area using the ROI Manager and

subsequently deleted from the total breast area using the Clear Outside function. For the majority of CC views, segmentation of the pectoral muscle is not required because it does not appear in the image, thus eliminating steps 3 and 4 shown in Fig. 1.

Another iteration of the k -means clustering routine was applied to the remaining breast area to segment the dense parenchyma as shown in Fig. 3(E). The operator can run the segmentation routine with different numbers of clusters and compare the results to the original parenchymal pattern shown in the mammogram. Furthermore, the user can alter the brightness and contrast features of the original mammogram to obtain an improved visualization of the breast's parenchymal pattern. By comparing the segmented image to the mammogram, the user will select the most suitable number of clusters on a mammogram by mammogram basis. As an example, the user can evaluate the performance of the clustering technique by selecting the clustered regions with the tracing tool and saving the ROI to the ROI Manager. This ROI can then be restored onto the original mammogram, and the overlay can provide information on the effectiveness of the clustering algorithm. For example, if the dense parenchymal area in the mammogram were smaller than the ROI, then an increase in the number of clusters would be required. Finally, the MPD was calculated as the segmented dense breast pixel area divided by the total breast pixel area (not including the chest wall) and subsequently converted into a percentage. One reader applied this technique to both CC and MLO views of the same breast for all 104 patients. To validate our technique, associations were investigated between BI-RADS category and calculated MPD for each mammographic view. A correlation was also made between the MLO and CC views. All statistical procedures were conducted using SPSS for Windows (version 15.0).

II.C. Reproducibility assessment

Next, to evaluate the reproducibility of mammographic segmentation, a randomly selected sample of eight patients was analyzed at five different time points separated by more than 2 days between each evaluation session. To prevent user bias, the observer was blinded to the previous time point's calculation. Because the patients were initially selected at random, were not arranged in a particular order, and the number of clusters varied for each patient, the potential of the operator recalling the number of clusters used for each patient was minimized. The means and standard deviations of the MPD were calculated for each patient. Further, the mean calculation time for the mixture modeling algorithm was calculated for all 40 measurements. Finally, a random sample of $\sim 10\%$ of the images was reanalyzed, and the intraclass correlation coefficient was determined.

III. RESULTS

III.A. Qualitative breast density measurements

Figure 4 shows three different mammograms segmented with our technique. Figure 4(a) shows a fatty breast (MPD

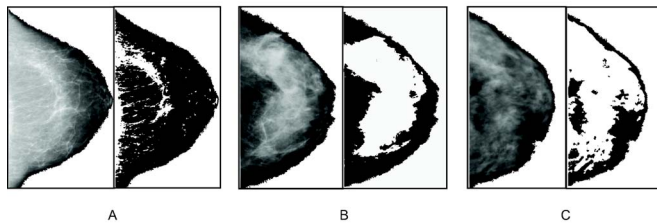


FIG. 4. Three different craniocaudal mammograms segmented with our in-house segmentation technique where the dense fibroglandular tissue appears in white and nondense portion of the breast appears in black. (A) A BI-RADS Category 1 breast with MPD \sim 15% using four clusters. (B) A BI-RADS Category 3 breast with MPD \sim 50% using three clusters. (C) A BI-RADS Category 4 breast with MPD \sim 70% using three clusters.

\sim 15%) calculated using four clusters, Fig. 4(b) is a heterogeneous breast (MPD \sim 50%) obtained with three clusters, and Fig. 4(c) is a dense breast (MPD \sim 70%), which was also segmented using three clusters. The pectoral muscle was segmented in all 104 MLO views. For the CC views, however, only 35% of the sample required the pectoral muscle to be removed.

Typically, the number of clusters used in segmentation is the same for similar BI-RADS Category breasts. For instance, seven out of eight dense breasts and seventeen out of nineteen heterogeneous breasts were segmented using three clusters. In general, the higher the number of clusters used, the lower the MPD for that particular breast. This generalization is further supported by the fact that the majority (ten out of eleven) of the BI-RADS 1 patients were segmented using greater than five clusters. The one patient who deviated from this trend had a calculated MPD of \sim 34% for both CC and MLO views, revealing that this patient should have actually been characterized as a BI-RADS Category 2 (scattered) breast.

Our technique was evaluated by comparing our results to the current standard of care: qualitative estimates using the BI-RADS Categorical Assessments. The resulting distribu-

tions are illustrated for both CC (Fig. 5 (left)) and MLO (Fig. 5 (right)) views. As expected, statistically significant correlations (two-tailed, $p < 0.01$) were observed between calculated MPD and BI-RADS for both CC (Spearman $\rho = 0.67$) and MLO views (Spearman $\rho = 0.71$). A one-way analysis of variance revealed that a significant difference existed between the mean values of calculated MPD according to BI-RADS ($p < 0.01$) for both views. For the CC views, further post hoc analyses using Scheffé criterion for significance ($\alpha = 0.05$) revealed that statistically significant differences existed between the mean MPD for each BI-RADS category except between fatty (BI-RADS 1) and scattered (BI-RADS 2). Finally, for the MLO views, statistically significant differences in the mean MPD between all BI-RADS Categories were observed.

III.B. Correlation of two mammographic views

Figure 6 shows the comparison of the calculated mammographic density for the MLO and CC views of the same breast for our sample of 104 patients. A strong positive correlation between the two views was demonstrated (Pearson $r = 0.8$). Linear regression yielded an equation of $y = 0.76x + 13.14$ to best describe the relationship between the two views, with a standard error of 0.06 and 2.09 in the slope and y intercept, respectively. There was a significant difference between MPD for the two mammographic views, $t(103) = 5.64$, $p < 0.001$, with the MLO views ($M = 39.2$, $SD = 13.8$) having higher MPD than the CC views ($M = 34.2$, $SD = 14.5$).

III.C. Reproducibility assessment

To characterize the reproducibility of our segmentation algorithm, one user calculated the MPD at five time points for eight different patients. Figure 7 shows the results for the mean MPD for each patient with one standard deviation shown by the error bars. The average standard deviation of MPD for all eight patients was 1.9% (range: 0.03%–9.9%).

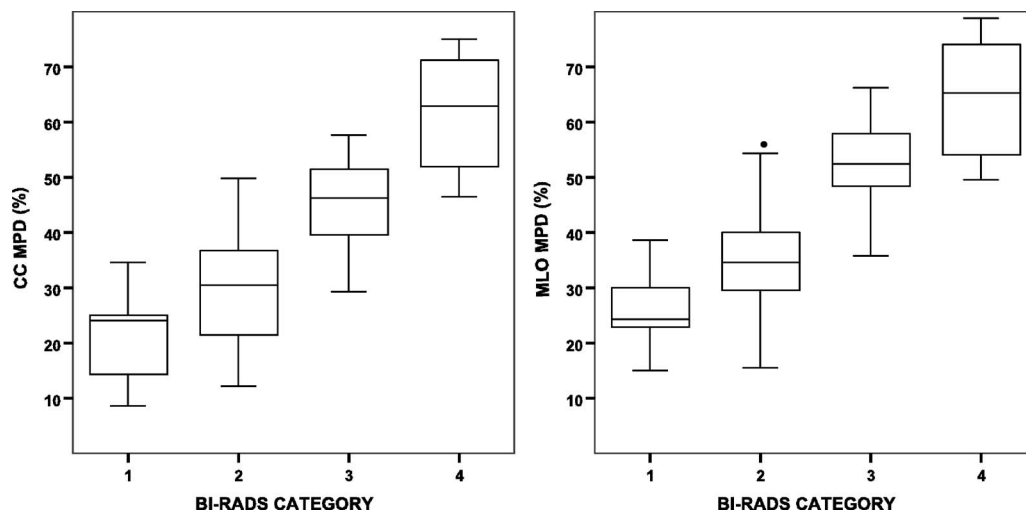


FIG. 5. The mammographic density calculated by our in-house segmentation method correlated with BI-RADS category for the CC (left) and MLO (right) views. Significant positive associations were found between the calculated mammographic percent density and BI-RADS category for both views.

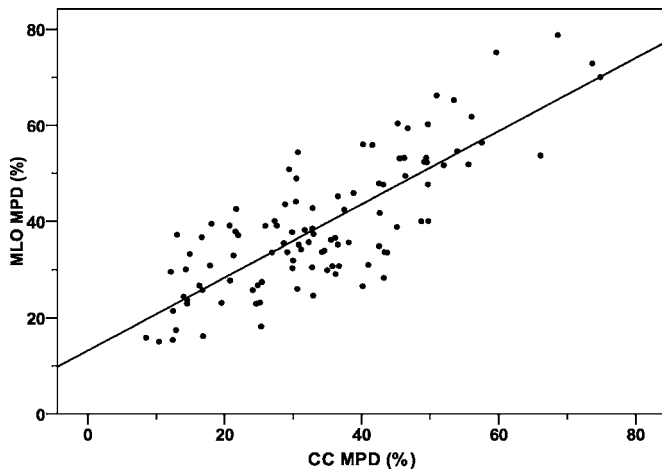


FIG. 6. A strong positive correlation was demonstrated (Pearson correlation =0.8) between CC and MLO views for our segmentation method ($n=104$).

The largest difference was observed for patient 7, where the number of clusters was misassigned by the observer for one out of five time points. This misassignment resulted in a MPD standard deviation of 9.9% for this patient case. Eliminating 1 misassignment out of the 40 calculations reduced the standard deviation to 0.35% for this patient, and the total overall average standard deviation for all eight patients was reduced to 0.75% (range: 0.03%–3.16%). The mean calculation time for the mixture modeling routine over all 40 segmented mammograms was 0.16 ± 0.02 s. A calculation time could not be computed for the k -means clustering technique; however, overall segmentation of dense tissue using the methodology outlined here is expected to take less than 30 s. Further, a random sample of $\sim 10\%$ of the images was re-analyzed, and the intraclass correlation coefficient was determined to be 0.80 and 0.85 for the CC and MLO views, respectively.

IV. DISCUSSION

In this feasibility study, we developed and evaluated a method for the quantitative analysis of mammograms that

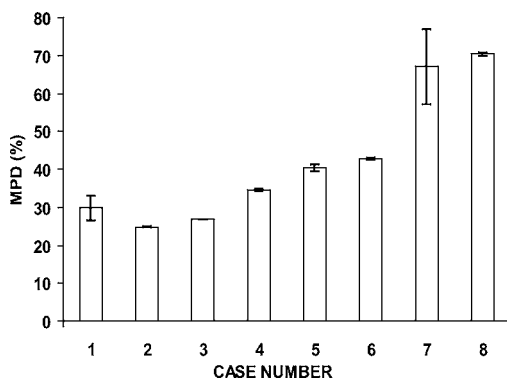


FIG. 7. The mammographic percent density calculated with our segmentation method for eight randomly selected patients at five different time points by the same observer. The error bars indicate one standard deviation of the mean.

automates the segmentation of the breast image from the background/radiographic markers and semiautomates the segmentation of the fibroglandular tissue from the rest of the breast. Our technique offers some unique advantages to assessing breast density. In particular, the user is required to define the number of clusters used in fibroglandular segmentation and evaluate the goodness of segmentation. While it was less advantageous to introduce user input, most methods of mammographic density calculation utilize interactive thresholding that requires the user to define two different gray-level values: one associated with dense tissue and one with the image background.^{15,17} Using these other approaches, the user must identify gray-level values for each, and evaluate the performance of each selection. Conversely, the method we have investigated involves the selection and evaluation of one user-defined parameter: the number of clusters. Therefore, this approach has the potential to provide more reproducible and less user-dependent MPD calculation. Both our methodology and other breast density evaluation methods require the user to determine if segmentation of the pectoral muscle is necessary, although our method implements the clustering technique to semiautomatically segment pectoral muscle present in all MLO views and as needed in CC views. This is a distinct advantage over other researchers' segmentation methods that require manual segmentation of the pectoral muscle,¹⁵ or use multiple straight edges to define an irregular boundary.²⁵ A clear advantage of quantitatively assessing breast density is the potential to develop a continuous evaluation scale that would be superior to the coarse BI-RADS categories.

Another group developed a computerized image analysis tool that segments the breast from the background using boundary tracking, reduces the gray-level range to enhance density differences, and classifies the breast based on the gray-level histogram for each image (i.e., MDEST).²⁶ While it is advantageous that this approach is fully automated, it does not always work because the histogram analysis method exhibited "gross misclassification" of 6% of the patient sample.²⁷ In addition, this technique was particularly problematic for distinguishing between women with fatty and dense breasts because of their similar gray-level histogram characteristics.²⁶ This was very disconcerting because using this methodology would characterize women with the highest breast cancer risk (BI-RADS Category 4) into the same category as the women with the least amount of risk (BI-RADS Category 1). Our method, on the other hand, automates breast detection from the background while semiautomating fibroglandular tissue segmentation. The implementation of a semiautomatic approach for dense tissue segmentation combines the benefits of automation with the discriminating power afforded by incorporating user input in an open-source and widely accessible software package. Presumably, MDEST is not commercially available at this time, and therefore extensive implementation may be limited. However, our segmentation technique utilizes IMAGEJ, public domain software developed with support from the National Institute of Health, and therefore has the potential to be readily put into practice. Not surprisingly, a major medical

data archiving corporation has embedded the IMAGEJ viewer into its DICOM media viewer, thus supporting the potential for widespread usage of the segmentation algorithms proposed here.²⁸

To compare our approach to the current standard of care, we arranged our calculated MPD results by BI-RADS compositional category, shown in Fig. 5. A statistically significant increase in calculated MPD and increasing BI-RADS breast density category was demonstrated for both mammographic views. Furthermore, for the MLO views, a statistically significant difference in the mean MPD between each BI-RADS category was demonstrated, whereas the CC views could not demonstrate significant differences between Categories 1 (fatty) and 2 (scattered). The binning of each BI-RADS category is coarse (i.e., 25% per category) and can also be related to intraobserver reliability. In addition, the overlap between the crucial categories of 2 (scattered) and 3 (heterogeneous) makes an objective determination of the 50% density level impractical for the designation of patients that may be considered for MRI screening. Despite the more objective nature of our technique, a spread in calculated MPD is expected for each BI-RADS category and was clearly demonstrated. Our investigation also involved only one reader, therefore eliminating the potential for interobserver variability. Overall, the strong positive correlation (Spearman $\rho \sim 0.7$ for both views) between MPD and BI-RADS category further validates our more operator-independent approach.

Several researchers have investigated the use of categorizing breast density with other classification schemes including the six-category classification,¹⁵ Wolfe's patterns,^{19,29} or Tabar's patterns.^{17,30} However, the American College of Radiology has established the BI-RADS compositional categories as the standard of care in clinical breast density reporting, which renders it the most clinically applicable approach. Further efforts were not made to evaluate the variability in the BI-RADS descriptor, particularly because this work has already been investigated by other researchers.^{13,14}

To further investigate our image segmentation methods, we correlated the results for the CC and MLO projections of the same breast. For the sample of 104 patients, a strong positive correlation was demonstrated (Pearson correlation = 0.8). Linear regression revealed $\sim 13\%$ offset in MPD for the MLO view compared to the CC view. However, MLO views are known to evaluate a greater extent of breast tissue, including more of the upper outer quadrant region where most cancers arise.^{31,32} Our results were consistent with MLOs evaluating more tissue area, due to the mean MPD for all 104 MLO views being about 5% higher (39%) than the mean MPD for all CC views (34%). Analyzing a single MLO view with our technique may thus be used for larger screening studies where effective time utilization may be important. Further, a perfect correlation between the two views cannot be expected for many reasons, including the variability in breast compression between views and the MLO projection inevitably incorporating a larger projected mammographic area. Limited data are available for similar

comparisons. One study by Byng *et al.* compared thresholded segmentation between CC and MLO views and revealed a correlation coefficient of 0.96 for two different observers.³³ However, this sample included only 30 patient mammograms evenly distributed among different breast densities. Our sample, on the other hand, had the majority of the data points concentrated at the same intermediate breast densities, with a sample over three times in size. As a result, the spread in the distribution adversely affected the correlation coefficient between views.

The reproducibility of our technique was assessed by one observer computing five repeated measures for eight patient cases. Including only one observer eliminated the potential for interobserver variability, and this approach was consistent with that of a recent study.⁴ The user selected a different number of clusters to evaluate a patient in only 1 out of 40 different calculations of MPD, and eliminating this misassignment resulted in less than 1% variability in our MPD calculations. This was slightly improved over results in a previous study where two radiologists misassigned the fibroglandular tissue density threshold in 1 out of 30 cases.³³ Further analysis of $\sim 10\%$ of the patient sample revealed strong agreement (ICC = 0.80–0.85) in the reliability of MPD estimates for both mammographic views. These results were lower than the 0.94 agreement demonstrated by Boyd *et al.*⁴ for CC views, although this was expected due to our sample being one-tenth the size. No comparisons were available to evaluate the reproducibility of our MLO segmentation technique, thus indicating the gap in knowledge of mammographic density estimation for this view. Overall, the reproducibility of quantitative measures is greatly improved over the intraobserver variability of BI-RADS category classification previously demonstrated.¹³

Although our results were encouraging, some limitations exist in our investigation. These include the coarse scale used in the BI-RADS category definition and having only one radiologist assess this parameter. Nevertheless, the purpose of this study was not to re-evaluate the BI-RADS descriptor, but rather to compare our mammographic segmentation technique to the current standard of care. Another limitation is the involvement of only one reader for quantitative image segmentation. This eliminated the potential for estimating interobserver variability for our pilot study, although this will be evaluated more extensively in future studies. Some major drawbacks of using film-screen mammography to assess breast density include the fact that it does not take into account breast thickness and relies on a 2D projection of a volume. While this may be true, mammography is the gold standard in breast cancer screening and detection, thereby making it most relevant for breast density evaluation. Our preliminary results have shown that our method for mammographic density estimation is consistent with current MPD assessments, although areas of future research include incorporating the variability of compressed breast volume, addressing differences in imaging parameters among patients and mammographic views, and estimating volumetric breast density. The clinical impact of our approach would be better determined in a larger clinical trial with a larger number of

readers and raters. With further development, a segmentation routine such as the one presented here could be readily incorporated into computer-aided diagnosis systems such as R2 Image Checker to calculate MPD for every patient and better identify women who are at elevated risk for breast cancer.³⁴

Recent attention has been given to incorporating breast density into breast cancer risk evaluation models.^{9–11} However, the effects of breast density on risk assessment have been shown to cause only marginal changes in calculated risk.^{9,11} This may be due in part to the coarseness of the current BI-RADS classification scheme, whereas a more quantitative breast density analysis such as the one presented here may reveal a more profound impact of breast density on breast cancer risk. Using our quantitative assessment to distinguish marginal changes in breast density will be explored in future longitudinal studies, which include investigating breast tissue response to treatment and chemoprevention.

V. CONCLUSIONS

The purpose of this paper was to introduce a technique for computer-assisted segmentation of breast density and to compare it to the current standard of care in breast density estimation (i.e., BI-RADS compositional categories). Our results suggest that our methods of evaluating breast density are consistent with the current standard of care, and demonstrated less intraobserver variability than BI-RADS categories. In addition, our technique showed a strong positive correlation between two different mammographic views, including the more representative MLO view. Finally, the intraobserver error was found to be less than 1% when one misassignment was excluded.

Our segmentation methods may be implemented for the objective referral of patients with sufficient risk to justify MRI screening (e.g., >50% MPD). In addition, the efficient utilization of our technique may objectively quantify slight changes in MPD caused by chemoprevention or dietary intervention to indicate potential reductions in breast cancer risk. Our methodology offers several advantages, which include automating the segmentation of the breast from the background and semiautomating the segmentation of the chest wall and fibroglandular tissue from the rest of the breast. Overall, this approach to evaluating breast density has the potential to provide a more quantitative means of evaluating breast density, thus better elucidating the relationship that exists between breast density and breast cancer risk.

ACKNOWLEDGMENTS

The authors would like to thank Olsi Rama for assistance in data processing, Lisa Bey-Knight for her help with patient recruitment, and Cuiping Li for sharing her software expertise. Furthermore, the authors wish to thank the staff of the Alexander J. Walt Comprehensive Breast Cancer Center at the Karmanos Cancer Institute for their generous assistance with patient management.

^{a)}Author to whom correspondence should be addressed. Electronic mail: glidec@karmanos.org. Telephone: 313-576-8313; Fax: 313-576-8767.

¹J. N. Wolfe, A. F. Saftlas, and M. Salane, "Mammographic parenchymal patterns and quantitative evaluation of mammographic densities: A case-control study," *AJR, Am. J. Roentgenol.* **148**, 1087–1092 (1987).

²N. F. Boyd, J. W. Byng, R. A. Jong, E. K. Fishell, L. E. Little, A. B. Miller, G. A. Lockwood, D. L. Tritchler, and M. J. Yaffe, "Quantitative classification of mammographic densities and breast cancer risk: Results from the Canadian National Breast Screening Study," *J. Natl. Cancer Inst.* **87**, 670–675 (1995).

³M. J. Yaffe, N. F. Boyd, J. W. Byng, R. A. Jong, E. Fishell, G. A. Lockwood, L. E. Little, and D. L. Tritchler, "Breast cancer risk and measured mammographic density," *Eur. J. Cancer Prev.* **7**, S47–55 (1998).

⁴N. F. Boyd, H. Guo, L. J. Martin, L. Sun, J. Stone, E. Fishell, R. A. Jong, G. Hislop, A. Chiarelli, S. Minkin, and M. J. Yaffe, "Mammographic density and the risk and detection of breast cancer," *N. Engl. J. Med.* **356**, 227–236 (2007).

⁵N. F. Boyd, G. A. Lockwood, J. W. Byng, D. L. Tritchler, and M. J. Yaffe, "Mammographic densities and breast cancer risk," *Cancer Epidemiol. Biomarkers Prev.* **7**, 1133–1144 (1998).

⁶V. A. McCormack and I. dos Santos Silva, "Breast density and parenchymal patterns as markers of breast cancer risk: A meta-analysis," *Cancer Epidemiol. Biomarkers Prev.* **15**, 1159–1169 (2006).

⁷C. Byrne, C. Schairer, J. Wolfe, N. Parekh, M. Salane, L. A. Brinton, R. Hoover, and R. Haile, "Mammographic features and breast cancer risk: Effects with time, age, and menopause status," *J. Natl. Cancer Inst.* **87**, 1622–1629 (1995).

⁸D. Saslow, C. Boetes, W. Burke, S. Harms, M. O. Leach, C. D. Lehman, E. Morris, E. Pisano, M. Schnall, S. Sener, R. A. Smith, E. Warner, M. Yaffe, K. S. Andrews, and C. A. Russell, "American Cancer Society guidelines for breast screening with MRI as an adjunct to mammography," *CA-Cancer J. Clin.* **57**, 75–89 (2007).

⁹J. Chen, D. Pee, R. Ayyagari, B. Graubard, C. Schairer, C. Byrne, J. Benichou, and M. H. Gail, "Projecting absolute invasive breast cancer risk in white women with a model that includes mammographic density," *J. Natl. Cancer Inst.* **98**, 1215–1226 (2006).

¹⁰M. R. Palomares, J. R. Machia, C. D. Lehman, J. R. Daling, and A. McTiernan, "Mammographic density correlation with Gail model breast cancer risk estimates and component risk factors," *Cancer Epidemiol. Biomarkers Prev.* **15**, 1324–1330 (2006).

¹¹W. E. Barlow, E. White, R. Ballard-Barbash, P. M. Vacek, L. Titus-Ernstoff, P. A. Carney, J. A. Tice, D. S. Buist, B. M. Geller, R. Rosenberg, B. C. Yankaskas, and K. Kerlikowske, "Prospective breast cancer risk prediction model for women undergoing screening mammography," *J. Natl. Cancer Inst.* **98**, 1204–1214 (2006).

¹²*BI-RADS Breast Imaging Reporting and Data System Breast Imaging Atlas* (American College of Radiology, Reston, VA, 2003).

¹³S. Ciatto, N. Houssami, A. Apruzzese, E. Bassetti, B. Brancato, F. Carozzi, S. Catarzi, M. P. Lamberini, G. Marcelli, R. Pellizzoni, B. Pesce, G. Risso, F. Russo, and A. Scorsolini, "Categorizing breast mammographic density: Intra- and interobserver reproducibility of BI-RADS density categories," *Breast J.* **14**, 269–275 (2005).

¹⁴W. A. Berg, C. Campassi, P. Langenberg, and M. J. Sexton, "Breast imaging reporting and data system: Inter- and intraobserver variability in feature analysis and final assessment," *AJR, Am. J. Roentgenol.* **174**, 1769–1777 (2000).

¹⁵J. W. Byng, N. F. Boyd, E. Fishell, R. A. Jong, and M. J. Yaffe, "The quantitative analysis of mammographic densities," *Phys. Med. Biol.* **39**, 1629–1638 (1994).

¹⁶M. Freedman, J. San Martin, J. O'Gorman, S. Eckert, M. E. Lippman, S. C. Lo, E. L. Walls, and J. Zeng, "Digitized mammography: A clinical trial of postmenopausal women randomly assigned to receive raloxifene, estrogen, or placebo," *J. Natl. Cancer Inst.* **93**, 51–56 (2001).

¹⁷N. Jamal, K. H. Ng, L. M. Looi, D. McLean, A. Zulfiqar, S. P. Tan, W. F. Liew, A. Shantini, and S. Ranganathan, "Quantitative assessment of breast density from digitized mammograms into Tabar's patterns," *Phys. Med. Biol.* **51**, 5843–5857 (2006).

¹⁸L. A. Venta, R. E. Hendrick, Y. T. Adler, P. DeLeon, P. M. Mengoni, A. M. Scharl, C. E. Comstock, L. Hansen, N. Kay, A. Coveler, and G. Cutter, "Rates and causes of disagreement in interpretation of full-field digital mammography and film-screen mammography in a diagnostic setting," *AJR, Am. J. Roentgenol.* **176**, 1241–1248 (2001).

¹⁹J. Brisson, C. Diorio, and B. Masse, "Wolfe's parenchymal pattern and

- percentage of the breast with mammographic densities: Redundant or complementary classifications?," *Cancer Epidemiol. Biomarkers Prev.* **12**, 728–732 (2003).
- ²⁰J. W. Byng, N. F. Boyd, E. Fishell, R. A. Jong, and M. J. Yaffe, "Automated analysis of mammographic densities," *Phys. Med. Biol.* **41**, 909–923 (1996).
- ²¹W. S. Rasband, "ImageJ," <http://rsb.info.nih.gov/ij/>.
- ²²C. Mei and M. Dauphin, "Mixture modeling," <http://rsb.info.nih.gov/ij/plugins/mixture-modeling.html>.
- ²³SourceForge.net, "IJ Plugins: Clustering," <http://ij-plugins.sourceforge.net/plugins/clustering/index.html>.
- ²⁴A. K. Jain and R. C. Dubes, *Algorithms for Clustering Data* (Prentice Hall, Englewood Cliffs, NJ, 1988).
- ²⁵M. J. Yaffe, "Cumulus3," Sunnybrook and Women's College Health Sciences Center, Toronto.
- ²⁶C. Zhou, H. P. Chan, N. Petrick, M. A. Helvie, M. M. Goodsitt, B. Sahiner, and L. M. Hadjiiski, "Computerized image analysis: Estimation of breast density on mammograms," *Med. Phys.* **28**, 1056–1069 (2001).
- ²⁷K. E. Martin, M. A. Helvie, C. Zhou, M. A. Roubidoux, J. E. Bailey, C. Paramagul, C. E. Blane, K. A. Klein, S. S. Sonnad, and H. P. Chan, "Mammographic density measured with quantitative computer-aided method: Comparison with radiologists' estimates and BI-RADS categories," *Radiology* **240**, 656–665 (2006).
- ²⁸"DICOM Media Creators," http://www.tdkvelocd.com/medical/support/pdf/DMC_brochure.pdf.
- ²⁹G. Torres-Mejia, B. De Stavola, D. S. Allen, J. J. Perez-Gavilan, J. M. Ferreira, I. S. Fentiman, and I. Dos Santos Silva, "Mammographic features and subsequent risk of breast cancer: A comparison of qualitative and quantitative evaluations in the Guernsey prospective studies," *Cancer Epidemiol. Biomarkers Prev.* **14**, 1052–1059 (2005).
- ³⁰I. T. Gram, E. Funkhouser, and L. Tabar, "The Tabar classification of mammographic parenchymal patterns," *Eur. J. Radiol.* **24**, 131–136 (1997).
- ³¹W. R. Deaton, Jr. and H. H. Bradshaw, "Carcinoma of the breast—Why the upper outer quadrant?," *Surgery (St. Louis)* **28**, 583–584 (1950).
- ³²J. S. Spratt and W. L. Donegan, *Cancer of the Breast* (Saunders, New York, 1967).
- ³³J. W. Byng, N. F. Boyd, L. Little, G. Lockwood, E. Fishell, R. A. Jong, and M. J. Yaffe, "Symmetry of projection in the quantitative analysis of mammographic images," *Eur. J. Cancer Prev.* **5**, 319–327 (1996).
- ³⁴"Mammography processing systems," http://www.r2tech.com/mammography/products/processing_systems.php.